



Solar collector tilt angle optimization for solar power plant setup-able sites at Western Himalaya and correlation formulation

Anchal Awasthi¹ · Mehmet Ali Kallioğlu² · Ashutosh Sharma³ · Anand Mohan⁴ · Ranchan Chauhan³ · Tej Singh⁵ 

Received: 21 July 2021 / Accepted: 26 March 2022 / Published online: 20 April 2022
© The Author(s) 2022

Abstract

Tilt angle optimization of the solar collector is essential to achieve maximum power output. In this study, the performance analysis of monthly and yearly optimum tilt angles has been carried out for solar power plant setup-able sites in the Western Himalayan region of India. A mathematic model has been used for optimum tilt angle assessment. Annual average performance enhancement for monthly optimum tilt angles is 10–11%, 5–7% and 4–6% from horizontal, tilted at the latitude and tilted at an optimum tilt angle, respectively. Validation of the results has been carried out by mounting a polycrystalline PV panel at one of the suggested plant setup-able sites ($\phi 30^{\circ} 51' 1.656''$, $L 77^{\circ} 3' 41.508''$). The percentage variations found in experimental results are 8.85, 9.13 and 14.09 from horizontal, tilted at the latitude and tilted at yearly optimum tilt angle PV panel, respectively. To generalize the obtained result, correlations in terms of latitude and declination angle have also been formulated for yearly and monthly optimum tilt angles, respectively. The preciseness of the developed correlations has been validated by statistical tools. The results from this study have also been compared with the results of some previous studies, and good agreement has been obtained.

Keywords Solar collector · Tilt angle optimization · Correlation · Experimental validation · Western Himalayan region · Statistical analysis

Abbreviations

ϕ	Latitude
L	Longitude
n	Julian day
δ	Declination angle
θ	Incidence angle
ω	Hour angle
θ_z	Zenith angle
ω_s	Sunset angle
β	Tilt angle

H	Insolation over a horizontal surface
R_B	The ratio of beam insolation on the tilted surface to a horizontal surface
H_o	Daily extraterrestrial insolation
k_T	Day's clearness ratio
G_{SC}	Global solar constant
H_d	Diffuse insolation over a horizontal surface
$H_{g,t}$	Aggregate insolation over the tilted surface
ρ_g	Reflection factor
$\beta_{opt,monthly}$	Monthly optimum tilt angle
$\beta_{opt,yearly}$	Yearly optimum tilt angle
PE	Performance enhancement
$AAPPE$	Annual average percentage performance enhancement
$POPE$	Power output performance enhancement
PO	Power output

✉ Tej Singh
sht@inf.elte.hu

¹ Centre for Energy and Environment, Dr B R Ambedkar NIT, Jalandhar, Punjab, India 144011

² Faculty of Technology, Batman University, Batman, Turkey 72100

³ Department of Mechanical Engineering, Dr B R Ambedkar NIT, Jalandhar, Punjab, India 144011

⁴ Department of Electrical Engineering, A. P. Goyal Shimla University, Shimla, India 171009

⁵ Savaria Institute of Technology, Eötvös Loránd University, Szombathely, Hungary 9700

Introduction

Energy is essential for every living being to sustain life. Conventional methods of electricity generation have many disadvantages that can be eradicated by utilizing renewable

energy resources. Among the renewable energy resources, solar energy is available in abundance and has a very large scope specifically in India [1–4]. About 58% of India's geographical area is incident by $5 \text{ kWhm}^{-2} \text{ day}^{-1}$ solar insolation [5]. National Solar Mission (NSM) has been launched in India on January 11, 2010, with a target of developing 20 GW of solar power by 2022 which is further revised on June 17, 2015, to increase the target to 100 GW from 20 GW. As of December 31, 2017, 17,052 MW of solar power is being developed in India [6]. Thus, India has a very vast opportunity for solar energy which is being mined at surging speeds. Solar energy can be directly converted into conventional forms of energy, i.e., thermal as well as electrical energy [7, 8]. Direct or indirect energy gains from solar radiation (global radiations) are integrated with active or passive heating systems. These systems aim to preserve energy sustainability and minimize heat losses. Experimental, theoretical and numerical research has been done in the literature on photovoltaic systems, solar still desalination systems, building-integrated photovoltaic systems (BIPV), building-integrated photovoltaic thermal (BIPV/T) and solar water heater system [9, 10]. One of the major complications with solar energy collection is that the solar radiations do not fall perpendicularly to the surface of the earth. In order to overcome this restraint, solar collectors are tilted to some angle which is called tilt angle. These tilt angles are a function of latitude and declination angle and have a very large impact on the total energy collection rate [11]. So, the potential of solar energy can be maximized by solar collector tilt angle optimization.

Various studies have been reported in the literature for solar collector tilt angle optimization and their related consequences. Calabro [12] developed an algorithm for optimum tilt angle determination and found that optimum tilt angle is a function of latitude angle at any location. Thakur and Chandel [13] calculated and implemented optimum tilt angle on 190 kWp grid-interactive solar power plant and found that total increase in energy yield is 25%, 28% and 29% at yearly, seasonal and monthly optimum tilt angles, respectively, in comparison with the fixed tilt angle of the plant. Awasthi et al. [14] evaluated the optimum tilt angle for latitude at Himachal Pradesh, India. The authors also formulated annual adjustment models for the practical implementation of these models. Authors reported that from the conventional system of setting the solar collector at a latitude angle, the system performance improved by 5.51%. Optimization of slope angle for two distinctive temperature regions of Iran to maximize the solar radiations was carried out by Abdolzadeh and Mehrabian [15]. An annual increment in performance of the solar collector of 7–8% for selected sites at monthly optimum tilt angles was reported by the authors. Similarly, Benghanem [16] calculated the monthly optimum tilt angles for Madinah, Saudi Arabia. De Bernardes

et al. [17] utilized a distinguishing approach for yearly and monthly optimum tilt angle determination at Argentina using neural networks. Abdulsalam et al. [18] carried out a study for solar insolation estimation for different models at Dhahran city, Saudi Arabia. The results revealed that the performance-enhanced through different models were 7%, 14%, 33% and 48% for yearly optimum, monthly optimum, single-axis and double-axis, respectively, in comparison with the horizontal solar collector. In another study, Soulayman and Sabbagh [19] computed tilt angle for tropical regions. An increment of 11–18% from the conventional method was reported in the study. The authors also revealed that the radiation received over solar collector tilted at monthly optimum tilt angle is approximately equal to the solar collector tilted at a daily optimum tilt angle. Siraki and Pillay [20] computed optimum tilt angles for different urban areas at different latitudes and found that tilt angle is a function of obstacles in an urban area also. The aforementioned studies demonstrate the optimum tilt angle assessment necessity for maximum solar radiation collection. For estimation of insolation over tilted solar collector, either isotropic or anisotropic models of solar radiation distribution are utilized [21, 22]. The incorrect results might be obtained by the inappropriate choice of these models and other assumptions. So for validation of obtained results, an experimental investigation is generally adopted by the researchers [23–25]. This signifies the importance of experimental validation of analytically obtained optimum tilt angle.

To generalize the obtained optimum tilt angle for a particular or range of latitudes, correlation development has been carried out by various scholars. As mentioned earlier, the tilt angle is a function of the latitude of a place and the declination angle of the year. Thereby, the reported correlations for optimum tilt angles are either dependent on latitude or declination angle. It has also been observed that the correlations developed for yearly optimum tilt angle are in terms of latitude angle and for monthly optimum tilt angles in declination or extraterrestrial solar radiations. Wessley et al. [26] formulated a mathematical model for optimum tilt angle for some Indian cities and developed a correlation for yearly optimum tilt angle based on latitude. In another study, Yadav and Chandel [27] evaluated optimum tilt angle for 26 cities of India and developed a yearly optimum tilt angle correlation as a function of latitude. Yadav and Malik [28] estimated the monthly optimum tilt angle for six Indian sites and developed a correlation in terms of declination angle. Similarly, many other researchers developed correlations for monthly and yearly optimum tilt angles at various latitudes [29, 30].

The aforementioned studies on solar collector tilt angle optimization are equally effective for small and large solar energy collection units. However, their significance increases with the increasing capacity of the solar power

plants. The site for a large solar power plant setup should be selected afterward its qualification around some criteria. A significant amount of land area is required for setting up a solar power plant. Chandel et al. [31] suggested that for installing 2.5 MW plant space required is almost 13.14 acres (1 acre = 4047 m²). Solar power plants can be installed in moderately hilly regions without any obstacles like a tree, scrub, etc. Additionally, it is also non-beneficiary to setup a solar power plant by decapitation of forests. Most of the recently presented studies on optimum tilt angle determination are carried out for urban areas without considering the suitability of the solar power plant. Therefore, sites for tilt angle optimization should be selected where chances are supreme and favorable for setting up a solar power plant in near future.

The literature survey suggests that the solar collector tilt angle optimization and site selection significantly affect the radiation collection rate and capacity of the solar power plants, respectively. However, most of the studies for tilt angle optimization have been reported for urban areas which are inappropriate for setting up solar power plants. So, the first objective of this study is to identify solar power plant setup-able sites in the Western Himalayan region of India. After site selection, the second objective is to evaluate the optimum tilt angle at monthly and yearly levels for the identified sites and their performance analysis. The isotropic diffuse radiation model has been utilized for evaluating the optimum tilt angle values. The literature review also suggests that the experimental validation of the analytically obtained optimum tilt angle is necessary for flawless predictions and operations. So, experimental validation of the obtained results at one of the selected sites is the third objective. Lastly, the correlation postulations for optimum

tilt angles and their statistical analysis is the final objective of the current work. The detailed methodology for achieving the mentioned objectives has been presented in the next section.

Methodology

Site selection and data assemblage

The Himalayas are the mountain range in southern Asia extending in India, Nepal, Pakistan, Afghanistan, Bhutan and China. Himachal Pradesh is a northern state of India which lies in the Western Himalayan region. The state has a significant amount of solar energy potential of 33.84 GWp [32]. Himachal Pradesh is a hilly region with an altitude range from 450 to 7026 m above sea level, and according to a forest survey of India, 27.12% area of Himachal Pradesh is forest covered [33]. So, in this study, nine such sites have been selected in Himachal Pradesh which can be used for solar power plant installation. The criterion for the selection of these sites is open scrub, degraded forest and barren rocky land. The types of land have been identified by the data provided by the wasteland maps from the Department of Land Resources, India (Fig. 1a) [34]. These sites with their coordinates, i.e., latitude and longitude along with the type of land areas, are shown in Table 1. These sites have been selected by local surveys and satellite image surveys on Google Maps [35]. The geographical locations of these sites are presented on the map in Fig. 1b. The Surface meteorology and Solar Energy (SSE) datasets provided by the National Aeronautics and Space Administration (NASA) [36] have been

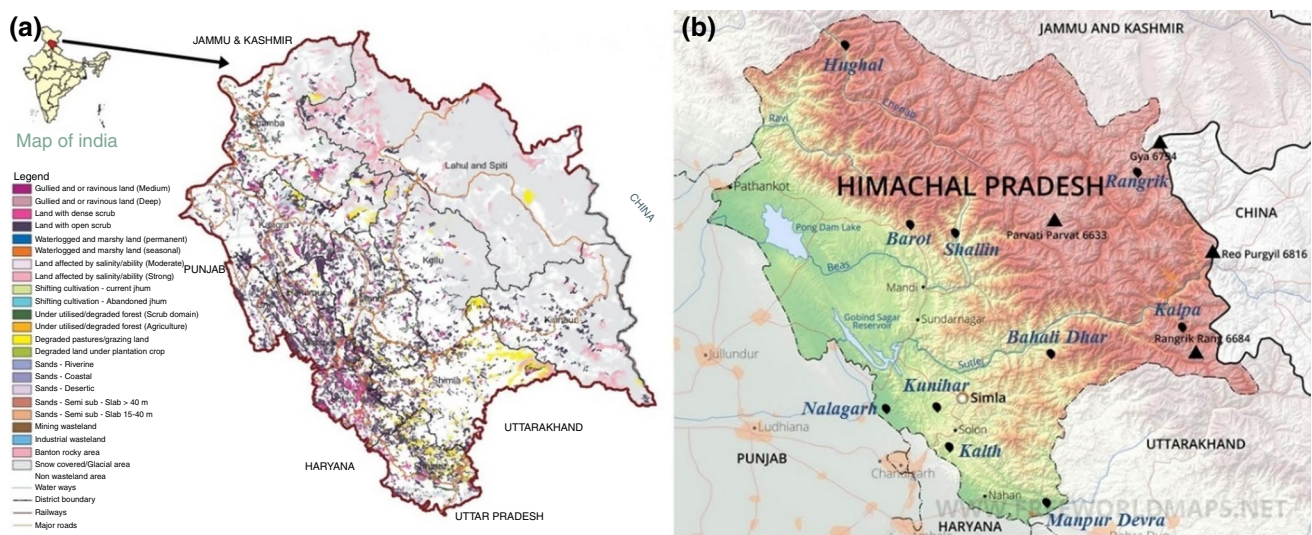


Fig. 1 a Wasteland map of Himachal Pradesh, b locations of selected sites on a geographical map

Table 1 Plant setup-able sites located in Himachal Pradesh with co-ordinates

S. No.	Place name	Latitude, ϕ/N	Longitude, L/E	District	Land type
1	Manpur Devra	30° 27' 9.648"	77° 41' 6.504"	Sirmour	Degraded forest (scrub domain)
2	Bahali Dhar	31° 25' 27.696"	77° 42' 24.804"	Shimla	Degraded Pastures
3	Shallin	32° 12' 15.372"	77° 8' 2.436"	Kullu	Land with open scrub
4	Rangrik	32° 14' 48.156"	78° 2' 11.724"	Lahaul and Spiti	Barren Rocky area
5	Barot	32° 2' 11.544"	76° 50' 52.692"	Mandi	Degraded pastures
6	Kalpa	31° 32' 25.08"	78° 14' 48.66"	Kinnaur	Land with open scrub
7	Hughal	33° 5' 33.216"	76° 24' 30.492"	Chamba	Land with dense scrub
8	Kalth	30° 51' 1.656"	77° 3' 41.508"	Solan	Degraded Pastures
9	Kunihar	31° 4' 42.456"	76° 58' 3.36"	Solan	Land with open scrub
10	Nalagarh	31° 1' 34.176"	76° 40' 57.54"	Solan	Land with open scrub

Table 2 Monthly average (2014–2017) global solar radiation data for different sites on the horizontal plane [36] ($\text{kWh m}^{-2} \text{day}^{-1}$)

Location	Month												Annual average
	Jan.	Feb.	Mar.	Apr.	May	Jun.	Jul.	Aug.	Sep.	Oct.	Nov.	Dec.	
Manpur Devra	3.12	4.21	5.09	6.34	6.68	5.97	4.48	4.71	5.12	4.96	3.96	3.25	4.82
Bahali Dhar	2.83	3.66	4.42	5.4	5.84	5.63	4.48	4.48	5.03	5.01	3.87	3.15	4.48
Shallin	3.06	4.19	5.15	6.84	7.65	5.85	5.58	5.38	5.56	5.32	3.7	3.07	5.11
Rangrik	3.41	3.95	5.34	7.39	8.10	6.81	6.10	6.14	6.14	5.68	4.19	3.37	5.56
Barot	2.55	3.24	3.79	4.65	5.46	5.50	4.44	4.55	4.90	4.80	3.49	2.84	4.18
Kalpa	3.28	4.12	5.22	7.00	6.10	6.10	5.36	5.35	5.64	5.30	4.06	3.17	5.06
Hughal	3.06	3.93	4.86	6.76	7.21	5.75	5.55	5.35	5.35	4.71	3.28	3.01	4.9
Kalth	3.12	4.21	5.09	6.34	6.68	5.97	4.48	4.71	5.12	4.96	3.96	3.25	4.82
Kunihar	2.98	4.01	4.91	6.18	6.73	6.15	4.85	4.95	5.23	4.91	3.82	3.15	4.81
Nalagarh	2.98	4.01	4.91	6.18	6.73	6.15	4.85	4.95	5.23	4.91	3.82	3.15	4.81

used for the data curation of solar radiation on the horizontal plane ($\text{kWh m}^{-2} \text{day}^{-1}$). The SSE provides $1^0 \times 1^0$ ($\sim 100 \times 100 \text{ km}$) spatial resolution data on a global grid with temporal coverage of solar radiation parameters for 22 years [37]. Global insolation data for the last four years have been taken for particular latitudes (ϕ). The monthly average of insolation data taken from SSE datasets for the 4 years (2014–2017) is shown in Table 2. Table 2 represents the variation in insolation for different sites at different months of the year and annual average insolation.

Optimum tilt angle assessment

The position of the sun changes over any specific location on earth throughout the year and even throughout the day because of the rotary and revolutionary motion of the earth around its axis and sun, respectively. Figure 2 represents the geometry of solar trajectory over a tilted surface placed over the earth’s surface along with different associated angles.

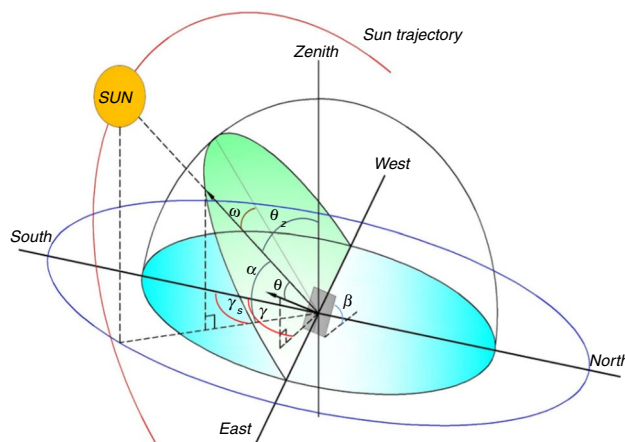


Fig. 2 Various angles w.r.t. sun over the tilted solar collector

Global insolation on a tilted surface ($H_{g,t}$) is an aggregation of three solar radiation components, i.e., direct, diffuse and reflected radiations. The $H_{g,t}$ can be calculated by Eq. 1 [38]:

$$H_{g,t}(\text{KWhm}^{-2}\text{day}^{-1}) = (H - H_d)R_B + H_d\left(\frac{1 + \cos\beta}{2}\right) + H \cdot \rho_g\left(\frac{1 - \cos\beta}{2}\right) \tag{1}$$

This shows that global insolation on the tilted surface is a function of global insolation on a horizontal surface (H), the ratio of the beam radiation on a tilted and horizontal surface (R_B), diffuse radiation on a horizontal surface (H_d), reflection factor (ρ_g) and tilt angle (β). Various models have been suggested in the literature for the estimation of diffuse radiation. Yadav and Chandel [27] investigated diffuse radiation estimation using different models at a northern location in India, and the results reveal that the isotropic diffuse radiation model suggested by Lui and Jordan [39] provides maximum solar insolation. Therefore, the same diffuse radiation estimation model has been used in the present study.

Data for global insolation on a horizontal surface (H) have been taken from the SSE datasets provided by NASA; R_B can be expressed as Eq. 2 [13],

$$R_B = \frac{\cos\theta}{\cos\theta_Z} = \frac{\cos(\phi - \beta)\cos\delta\sin\omega_s + \omega_s\sin(\phi - \beta)\sin\delta}{\cos\delta\sin\omega\cos\phi + \omega_s\sin\phi\sin\delta} \tag{2}$$

where θ , θ_Z , δ and ω_s are incidence angle, zenith angle, declination angle and sunset angle, respectively. The expressions for calculating δ and ω_s are as follows [40],

$$\delta = 23.45\sin\left(360\frac{284 + n}{365}\right) \tag{3}$$

$$\cos\omega_s = -\frac{\sin\phi\sin\delta}{\cos\phi\cos\delta} = -\tan\phi\tan\delta \tag{4}$$

H_d is a function of the clearness ratio (k_T) and H . H_d is given by,
for $\omega_s \leq 81.4^\circ$

$$\frac{H_d}{H} = 1.391 - 3.56k_T + 4.189k_T^2 - 2.137k_T^3$$

and for $\omega_s \geq 81.4^\circ$

$$\frac{H_d}{H} = 1.311 - 3.022k_T + 3.427k_T^2 + 1.821k_T^3 \tag{5}$$

where, $k_T = H/H_0$. H_0 is extraterrestrial radiations on a horizontal surface, and for any Julian day (n) of the year, it is evaluated as Eq. 6, where G_{SC} is the global solar constant ($G_{SC} = 1367 \text{ Wm}^{-2}$) [22].

$$H_0(\text{KWhm}^{-2}\text{day}^{-1}) = \frac{24 \times G_{SC}}{\pi} \left(1 + \left(0.033\cos\left(\frac{360n}{365}\right)\right)\right) \tag{6}$$

The optimum value of β lies in the range of $0^\circ \leq \beta \leq 90^\circ$. Therefore, for finding the optimum tilt angle corresponding to maximum $H_{g,t}$ for a particular latitude, the value of β has been varied from 0 to 90 degrees. Performance enhancement (PE) of the solar collector tilted at $\beta_{opt, monthly}$ from otherwise tilted is expressed by Eq. 7.

$$PE(\text{age}) = \left(\frac{(H_{g,t})_{\beta_{opt,monthly}} - (H_{g,t})_{\beta}}{(H_{g,t})_{\beta_{opt,monthly}}}\right) \times 100 \tag{7}$$

Experimental validation

The experimental analysis has been conducted at one of the selected sites [Kalth ($\phi 30.85^\circ$, $L 77.06^\circ$)] to validate the obtained analytical results of optimum tilt angle. A polycrystalline PV panel fixed on a tilt-able stand facing toward the true south has tilted at different angles. The tilt-able stand was designed to fix four options of horizontal, latitude, yearly optimum and monthly optimum tilt angles. Specifications of the PV panel used for experimental validation are shown in Table 3. A pictographic view of the tilt-able panel and circuit diagram is shown in Fig. 3.

Hourly data for open-circuit voltage (VOC) and short-circuit current (ISC) have been recorded. Power output (PO) from the panel is recorded as Eq. 8,

$$PO = V_{OC} \times I_{SC} \tag{8}$$

Percentage gain in power output is termed as power output performance enhancement ($POPE$) and calculated by Eq. 9.

$$POPE = \left(\left(\frac{(PO)_{\beta_{opt,monthly}} - (PO)_{\beta}}{(PO)_{\beta_{opt,monthly}}}\right) \times 100\right) \tag{9}$$

POPE at a particular location and time represents PE. So, to validate the obtained results the PE has been compared with POPE and percentage variation is calculated by Eq. 10.

Table 3 Specifications of the polycrystalline PV panel

Parameter	Units	Magnitude
P_{max}	W	74
Voltage (V_{max})	V	18
Current (I_{max})	A	4.25
Open-circuit voltage (VOC)	V	21
Short-circuit current (ISC)	A	4.55
Bypass diode rating	A	8
System voltage	V (DC)	1000
Safety class	-	II

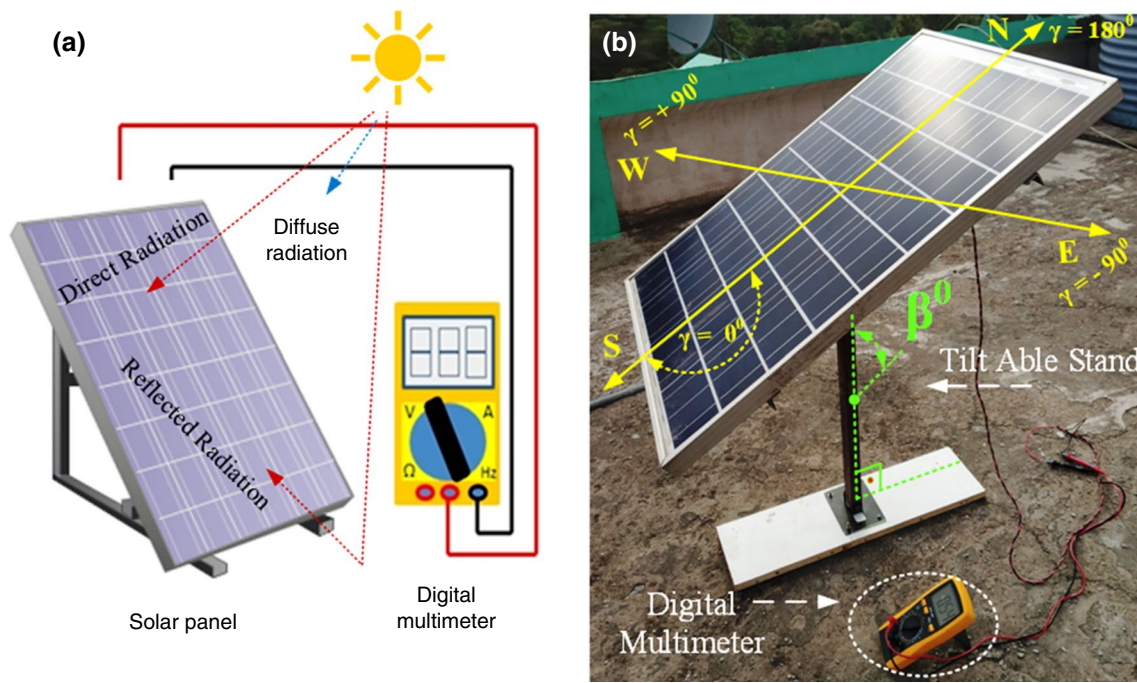


Fig. 3 Circuit diagram (a) and pictographic view (b) of the experimental setup

This percentage variation has been used as a validating tool for this study.

$$\text{Percentage Variation} = \left(\left(\frac{(PE)_\beta - (POPE)_\beta}{(PE)_\beta} \right) \times 100 \right) \tag{10}$$

Correlations for optimum tilt angles

The current section discusses the methodology adopted for correlation formulation. The calculation part consists of two stages. The first stage includes the formulation of three mathematical models for optimum tilt angle estimation as a function of the declination angle of the selected sites. Declination angle is computed by Eq. 3; as is known, it changes by the rotation of the earth around the sun. Table 4 shows the recommended monthly declination angle value corresponding to the Julian days. The latitude of sample cities that were used in the calculation is between 30° 30' N- (lowest) and 33° 6' N (highest). Therefore, mathematical models (Eqs. 15–17) have been

established based on the declination angle which can completely answer the selected area.

In the second stage, three different mathematical correlations for yearly optimum tilt angle based on latitude have been developed. The yearly optimum tilt angle of any site in the selected latitude range can be calculated utilizing the established equations. The accuracy of the developed correlations from stages 1 and 2 has been checked using the statistical comparison methods.

Statistical methods

The investigation of the correlation accuracy is necessary for increasing the frequent usability of the developed mathematical models. Literature has demonstrated numerous methods to determine the statistical accuracy of developed equations. The most commonly used methods are mean bias error (MBE), root-mean-square error (RMSE) and t-statistics (t-sat). The main goal of these methods is to find the usability and accuracy of mathematical correlations [40, 41]

Table 4 Recommended average day and declination for each month

Months	Jan.	Feb.	Mar.	Apr.	May	Jun.	Jul.	Aug.	Sep.	Oct.	Nov.	Dec.
Day of the year	17	47	75	105	135	162	198	228	258	288	318	344
Date	17	16	16	15	15	11	17	16	15	15	14	10
Declination (δ)	- 20.92	- 13.29	- 2.42	9.41	18.79	23.09	21.18	13.45	2.22	- 9.60	- 18.91	- 23.05

MBE informs on long-term values of correlation. Minimum value implies more effectiveness of correlation, and the ideal value is being close to zero. It is calculated by Eq. 11. ci (calculated) in the equation represents the computed value; mi (measured) shows the measured value.

$$MBE = \frac{1}{n} \sum_{i=1}^n (mi - ci) \quad (11)$$

The RMSE is a statistical tool that has importance in terms of comparing both short-run measured and estimated performance. It always takes a positive value. The most ideal value is closest to zero. It is expressed by Eq. 12.

$$RMSE = \sqrt{\frac{1}{n} \sum_{i=1}^n (ci - mi)^2} \quad (12)$$

The t-test method (t-stat) is decided whether the difference between the t-test and the average of two groups is accidental or statistically rational [42]. It is shown in Eq. 13.

$$t - stat = \sqrt{\frac{(n - 1)MBE^2}{RMSE^2 - MBE^2}} \quad (13)$$

The power of connection between two variables can be evaluated using the determination coefficient (R^2). It is used to specify the linear relationship between computed and measured data. The value of this coefficient varies between 0 and 1 ($0 < R^2 < 1$), and the most ideal value is the closest to zero. It is expressed by Eq. 14; ca and ma are the averages of, respectively, computed and measured values.

$$R^2 = \frac{\sum_{i=1}^n (ci - ca)x(mi - ma)}{\left[\sqrt{\sum_{i=1}^n (ci - ca)^2} \right] x \left[\sqrt{\sum_{i=1}^n (mi - ma)^2} \right]} \quad (14)$$

Results and discussion

Tilt angle assessment and performance enhancement

Monthly optimum tilt angles for selected sites have been computed utilizing Eq. 1–7. Figure 4 shows the radiation intensity corresponding to the different tilt angles (0° – 90°) for selected sites. The results depict that the optimum tilt angles corresponding to the maximum solar radiations lie in the range of 0 – 56° for all the selected sites. The highest optimum tilt angle values can be observed in December–January, while the lowest values are in May–July. While solar panel tilt angle values are in a decreasing trend in the period from December to June, it tends to increase in the period from June to December. In the northern hemisphere,

the sun's rays come at the right angle on June 21, while the opposite happens on December 21 at the maximum oblique angle as a result of the annual movement of the earth. The tilt angle which facilitates maximum insolation has been selected as $\beta_{opt,monthly}$. The result depicts that the monthly optimum tilt angle ($\beta_{opt,monthly}$) varies from 47° to 55° in January, 43° – 48° in February, 31° – 37° in March, 16° – 19° in April, 0° for May–July, 8° – 10° degrees for August, 27 – 30° in September, 44° – 48° in October and 51° – 56° in November and December for all the selected solar plant setup-able sites. The range of monthly optimum tilt angles for different sites is shown in Fig. 5. It is generally known by researchers that the optimum slope depends on the latitude and day of the year. Throughout the year, the panel inclination angle is taken equal to latitude (ϕ); it is taken more than latitude ($\phi + 15$) in winter and lower than latitude ($\phi - 15$) in summer [38, 43, 44]. Figure 6 shows the solar radiations corresponding to solar collector tilted at annual average, latitude, horizontal and monthly optimum for all regions. The figure depicts that the solar collector tilted at monthly optimum tilt angle receives maximum solar radiations as compared to other positions. Performance enhancement (PE) of the tilted solar collectors to $\beta_{opt,monthly}$ is measured by comparing it with horizontal, tilted at the latitude and tilted at yearly optimum tilt angle solar collectors. Equation 8 is utilized for the comparison, and the results are presented in supplementary data.

The PE is maximum in October–March and minimum in April–August from the horizontally aligned solar collector. This is because the optimum tilt angle for April–August is very small approaches toward zero. PE for $\beta = \phi$ and $\beta_{opt,yearly}$ is minimum ($< 5\%$) in March–April and August–October. Annual average percentage performance enhancement (AAPPE) is plotted in Fig. 7 which follows the order of (AAPPE) $\beta = 0^\circ > (AAPPE) \beta = \phi > (AAPPE) \beta = \beta_{opt,yearly}$ for all the selected sites. This shows that PE is maximum from $\beta = 0^\circ$ then $\beta = \phi$ and least from $\beta = \beta_{opt,yearly}$. So, for collecting maximum solar radiations, the solar collector should be tilted in order of, $\beta_{opt,monthly} > \beta_{opt,yearly} > (\beta = \phi) > (\beta = 0^\circ)$.

Experimental validation

Validation of the obtained results has been carried out by adjusting the tilt angle of a PV panel to different positions at one of the selected locations, i.e., Kalth ($\phi 30^\circ 51' 1.656''$, $L 77^\circ 3' 41.508''$). Experimentation has been carried out from 17/03/2019 to 31/03/2019, and data have been recorded for open-circuit voltage (V_{OC}) and short-circuit current (I_{SC}) of the PV panel. PV panel has been tilted to four positions, $\beta_{opt,monthly}$ (i.e., 37°), $\beta_{opt,yearly}$ i.e., 28.83° , ϕ , i.e., $30^\circ 51' 1.656''$, and horizontal (0°). Daily variation in average

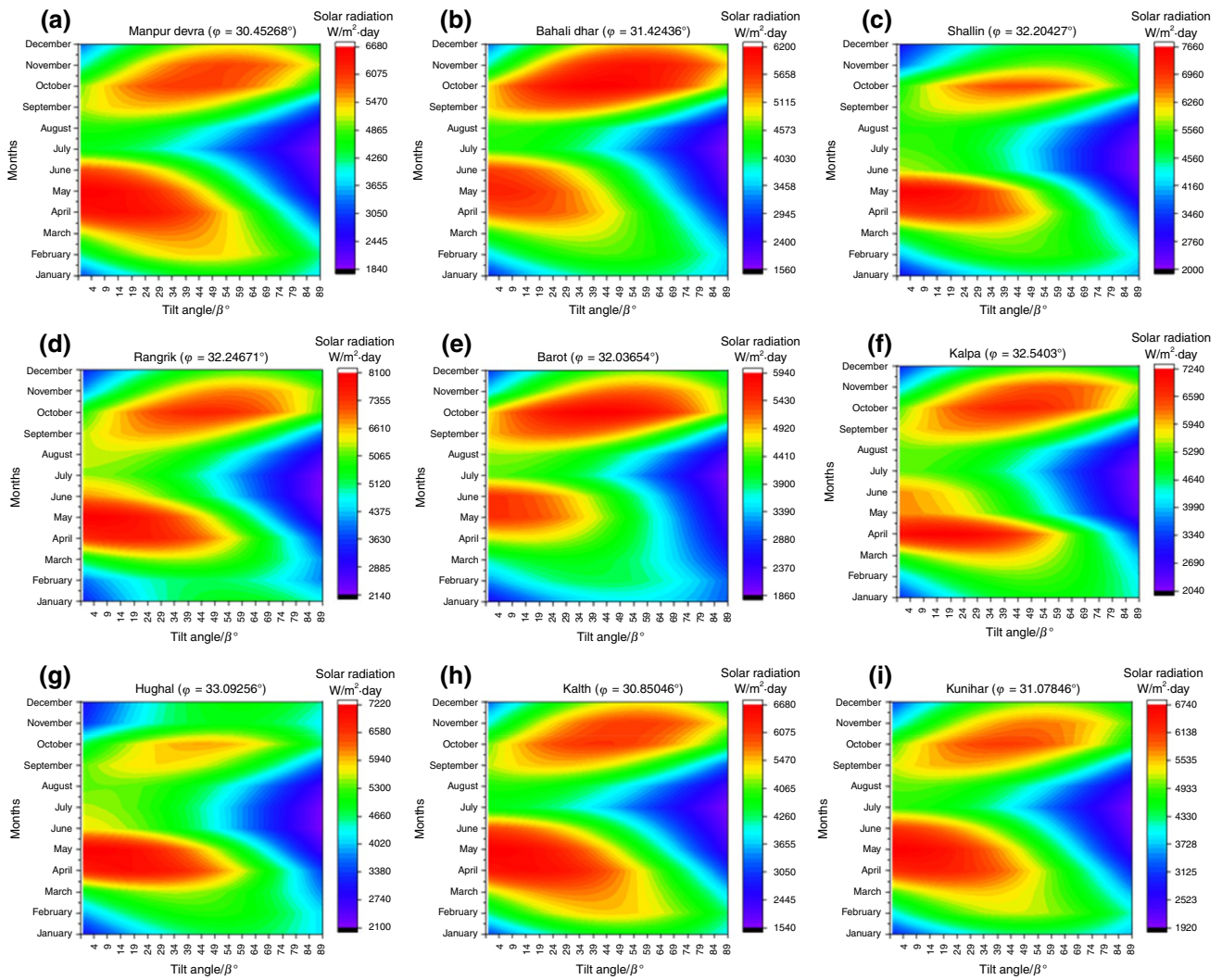


Fig. 4 Monthly optimum solar tilt angle change **a** Manpur Devra, **b** Bahali Dhar, **c** Shalin, **d** Rangrik, **e** Barot, **f** Kalpa, **g** Hughal, **h** Kalth, **i** Kunihar

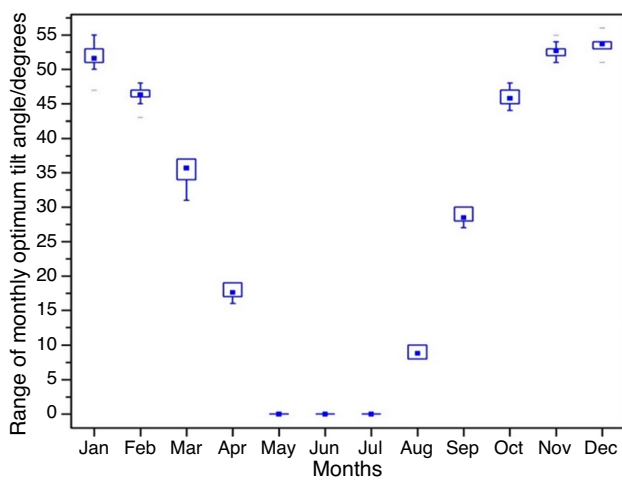


Fig. 5 Monthly optimum tilt angle range for different sites

power output (PO) for differently tilted PV panels is shown in Table 5.

Equation 10 is used for evaluating the power output performance enhancement (POPE). The POPE for $\beta_{opt, monthly}$ from, $\beta = \phi$, $\beta_{opt, yearly}$ and 0° is found to be 0.1453%, 0.335% and 10.28%, respectively. POPE represents PE for a particular month, and to validate the results the POPE is compared with the computed PE values at Kalth. Table 6 represents the comparison of POPE and PE. The percentage variation (from Eq. 11) of the POPE from PE for $\beta = 0^\circ$, $\beta = \phi$ and $\beta = \beta_{opt, yearly}$ is 8.84%, 9.13% and 14.05%, respectively. These results are found very much closer (i.e., <15% variation) to the proposed numerical results. The variation among POPE and PE can be justified as different climatic conditions and losses at particular tilt positions of the PV panel. Figure 8 shows that PO of PV panel tilted at $\beta_{opt, monthly}$ goes on decreasing comparatively

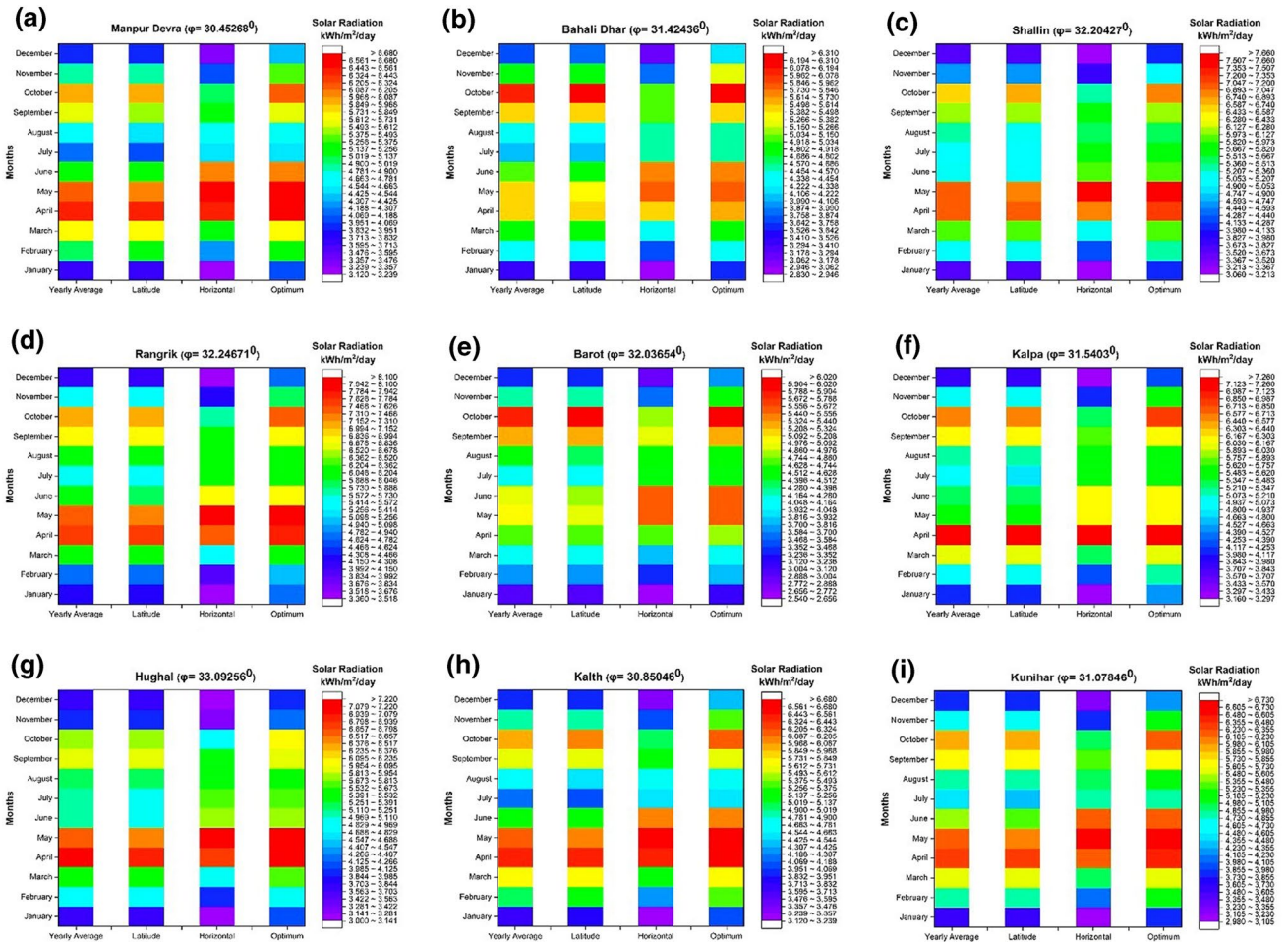


Fig. 6 Solar radiation corresponding to different tilt angles at a Manpur Devra, b Bahali Dhar, c Shalin, d Rangrik, e Barot, f Kalpa, g Hughal, h Kalth, i Kunihar

Fig. 7 Annual average percent-age performance enhancement (AAPPE) for selected sites

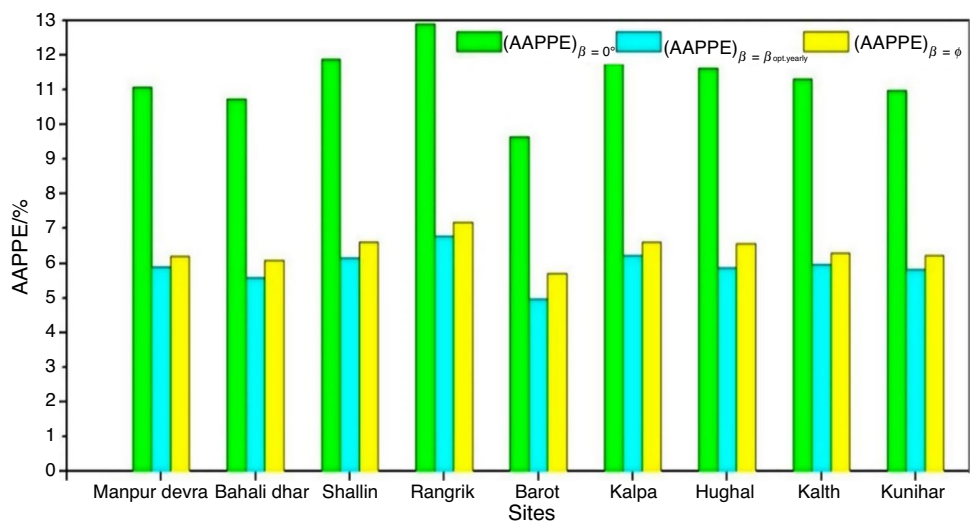


Table 5 Daily average power output of PV panel tilted at different tilt angles

Day No.	Julian day (<i>n</i>)	Date	Power output for $\beta = \beta_{opt,monthly}$ (W)	Power output for $\beta = \beta_{opt,yearly}$ (W)	Power output for $\beta = 0^0$ (W)	Power output for $\beta = \phi$ (W)
1	76	17/03/2019	59.0	54.6	49.4	55.5
2	77	18/03/2019	58.5	54.8	49.5	55.7
3	78	19/03/2019	58.8	55.7	50.4	56.5
4	79	20/03/2019	58.3	56.0	50.5	56.5
5	80	21/03/2019	57.2	55.6	50.0	56
6	81	22/03/2019	56.5	55.5	49.9	55.9
7	82	23/03/2019	56.2	56.0	50.2	56.2
8	83	24/03/2019	55.5	56.0	50.1	56.2
9	84	25/03/2019	55.2	56.4	50.3	56.6
10	85	26/03/2019	55.0	56.6	50.4	56.5
11	86	27/03/2019	55.8	57.1	51.1	56.8
12	87	28/03/2019	55.3	57.0	51.2	56.5
13	88	29/03/2019	54.9	56.9	51.3	56.3
14	89	30/03/2019	54.3	56.8	51.4	56.1
15	90	31/03/2019	53.8	56.7	51.5	56
Average power output (W)			56.2626	56.0741	50.4775	56.1808
POPE			–	0.335%	10.28%	0.1453%

Table 6 Comparison of POPE and PE for March at Kalth

Parameter	For $\beta = 0^0$ (%age)	For $\beta = \beta_{opt, yearly}$ (%age)	For $\beta = \phi$ (%age)
PE	11.28	0.39	0.16
POPE	10.28	0.335	0.1453
% Variation	8.84	14.09	9.13

as we proceed to the end of the month. This trend is due to the fact that $\beta_{opt, monthly}$ for April is smaller, i.e., 17^0 . The trend for power output from PV panels tilted at latitude is of domed shape which increases for the first few days and decreases in some last days. For PV panels tilted at $\beta_{opt, yearly}$, PO shows the almost same trend as tilted at latitude angle because of a very small difference among latitude and yearly optimum tilt angles. For horizontal PV panel, the daily average power output is increasing gradually because the optimum tilt angle approaches toward $\beta_{opt, monthly}$ of April.

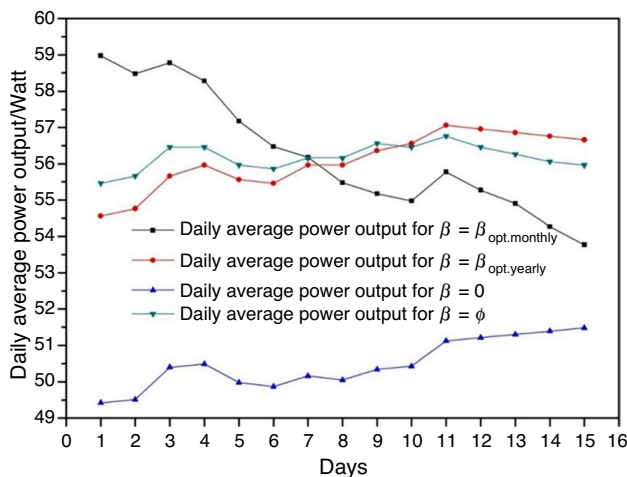


Fig. 8 Average daily variation of the power output of PV panel tilted at latitude, monthly optimum tilt angle and horizontal

The correlations for solar collector optimum tilt angles

The correlations have been developed for the monthly and yearly optimum tilt angles for the selected sites in order to generalize the obtained results. Initially, the linear, second-degree polynomial and third-degree polynomial correlations were developed by using the declination angle (δ) for the monthly optimum tilt angle at the Kalth. Equations 15–17 represent the developed correlations for linear, second-degree and third-degree polynomial, respectively. The results are presented in Fig. 9a.

$$\beta_{opt,monthly} = -1.2949(\delta) + 28.365 \tag{15}$$

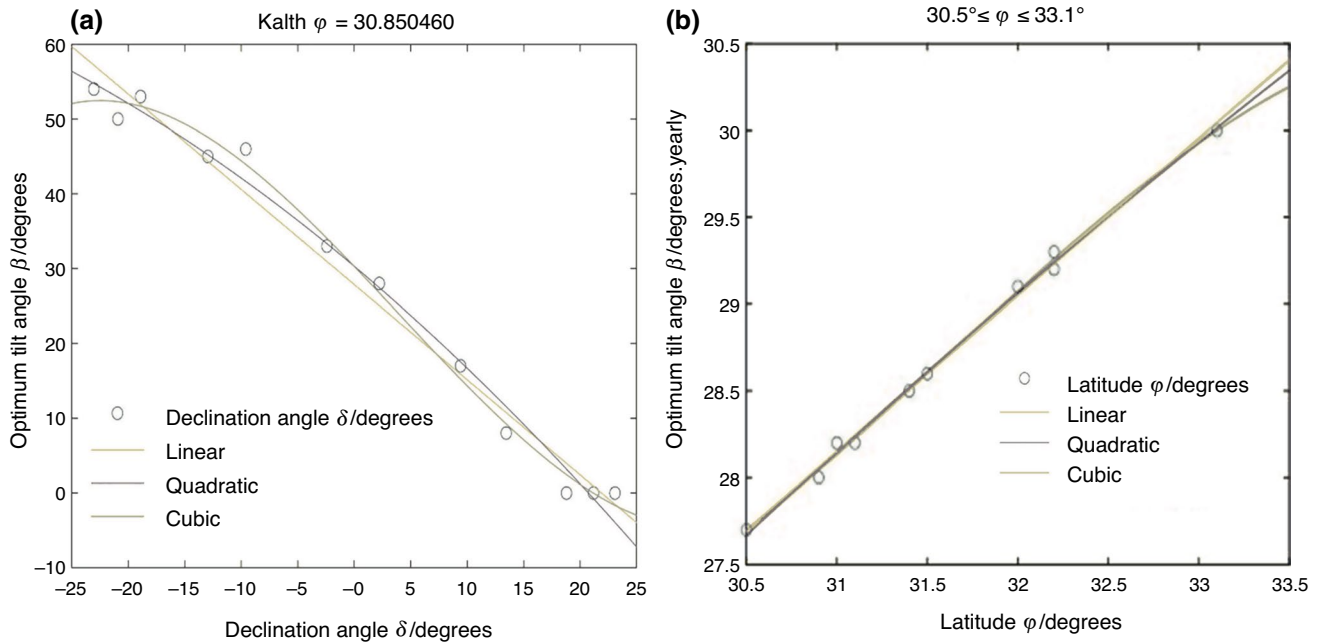


Fig. 9 Curve fitting for a $\beta_{opt, monthly}$ at Kalth, b $\beta_{opt, yearly}$ at selected sites

$$\beta_{opt,monthly} = -0.0102(\delta)^2 - 1.2936(\delta) + 31.093 \quad (16)$$

$$\beta_{opt,monthly} = 0.0009(\delta)^3 - 0.0102(\delta)^2 - 1.6462(\delta) + 31.07 \quad (17)$$

$$\beta_{opt,yearly} = 0.9033(\phi) + 0.146 \quad (18)$$

$$\beta_{opt,yearly} = -0.0002(\phi)^2 + 0.913(\phi) \quad (19)$$

$$\beta_{opt,yearly} = -0.0008(\phi)^3 + 0.0511(\phi)^2 + 0.099(\phi) \quad (20)$$

The practicality of monthly optimum tilt angle is depreciated due to tediousness and cost involvement. This difficulty can be overcome by yearly optimum tilt angle up to some extent. So, three different mathematical models based on latitude were developed to determine the yearly optimum solar collector tilt angle. Equations 18–20 used for a selected range of latitude ($30^{\circ} 30' \leq \phi \leq 33^{\circ} 6'$) as seen in Fig. 9b. The yearly optimum solar panel tilt angle can be estimated based on the latitude using these mathematical models. The next

section discusses the statistical analysis of these developed models.

Statistical analysis for developed models

Table 7 statistically shows the success of mathematical models to estimate monthly and yearly optimum angles. Estimation equations that give best results in terms of R^2 (determination coefficient), respectively, are Eq. 15 (0.9795), Eq. 16 (0.9878), Eq. 17 (0.9960) for Kalth and Eq. 18 (0.9960), Eq. 19 (0.9961), Eq. 20 (0.9966) for $30^{\circ} 30' N-33^{\circ} 6' N$. Mean bias error (MBE) statistical method data, respectively, are Eq. 15 (0.0005), Eq. 16 (-0.0061), Eq. 17 (-0.0113) for Kalth and Eq. 18 (-0.0012), Eq. 19 (0.0380), Eq. 20 (-0.2081) for $30^{\circ} 30' N-33^{\circ} 6' N$. Root-mean-square error (RMSE) statistical method, respectively, is Eq. 17 (1.3631), Eq. 16 (2.3582), Eq. 15 (3.0574) for Kalth and Eq. 18 (0.0420), Eq. 19 (0.0566), Eq. 20 (0.2122) for $30^{\circ} 30' N-33^{\circ} 6' N$. The t-stat (t-statistics), respectively, are Eq. 15 (0.0005), Eq. 16 (0.0086), Eq. 17 (0.0275) for Kalth and Eq. 18 (0.0985), Eq. 19 (3.0024), Eq. 20 (16.6257) for

Table 7 Statistical analysis of developed equations for Kalth and ($30^{\circ} 30' \leq \phi \leq 33^{\circ} 6'$)

	Kalth			30.50 N- 33.10 N		
	Equation 15	Equation 16	Equation 17	Equation 18	Equation 19	Equation 20
R^2	0.9795	0.9878	0.9960	0.9960	0.9961	0.9966
MBE	0.0005	-0.0061	-0.0113	-0.0012	0.0380	-0.2081
RMSE	3.0574	2.3582	1.3631	0.0420	0.0566	0.2122
t-stat	0.0005	0.0086	0.0275	0.0985	3.0024	16.6257

Table 8 The developed cubic correlations for different sites and their statistical analysis

Site	Correlations	Statistical analysis			
		R^2	MBE	RMSE	t-stat
Manpur Devra	$\beta_{OPT} = 0.0008(\delta)^3 - 0.0086(\delta)^2 - 1.5987(\delta) + 30.222$	0.9959	- 0.0039	1.3619	0.0096
Bahali Dhar	$\beta_{OPT} = 0.0008(\delta)^3 - 0.0092(\delta)^2 - 1.5818(\delta) + 30.293$	0.9932	0.0014	1.7486	0.0026
Shallin	$\beta_{OPT} = 0.0008(\delta)^3 - 0.0139(\delta)^2 - 1.6008(\delta) + 32.966$	0.9961	- 0.0005	1.3614	0.0011
Rangrik	$\beta_{OPT} = 0.0007(\delta)^3 - 0.0116(\delta)^2 - 1.5983(\delta) + 32.861$	0.9946	- 0.0051	1.6319	0.0103
Barot	$\beta_{OPT} = 0.0008(\delta)^3 - 0.0108(\delta)^2 - 1.5296(\delta) + 29.721$	0.9897	- 0.0010	2.0362	0.0016
Kalpa	$\beta_{OPT} = 0.0008(\delta)^3 - 0.0122(\delta)^2 - 1.6431(\delta) + 32.273$	0.9957	- 0.0100	1.4446	0.0229
Hughal	$\beta_{OPT} = 0.0006(\delta)^3 - 0.0131(\delta)^2 - 1.5077(\delta) + 32.349$	0.9952	- 0.0077	1.4631	0.0174
Kunihar	$\beta_{OPT} = 0.0009(\delta)^3 - 0.0118(\delta)^2 - 1.6149(\delta) + 31.249$	0.9953	- 0.0142	1.4680	0.0321
Nalagarh	$\beta_{OPT} = 0.0009(\delta)^3 - 0.0118(\delta)^2 - 1.6149(\delta) + 31.249$	0.9953	- 0.0142	1.4680	0.0321

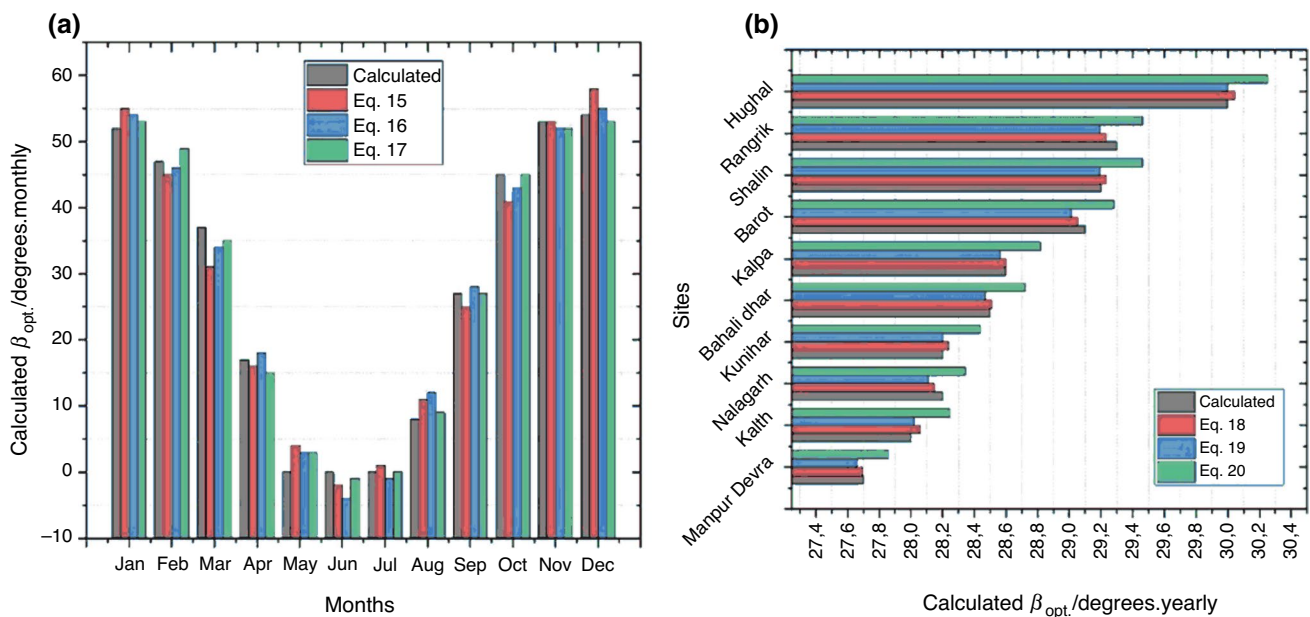


Fig. 10 Calculated and predicted values comparison for **a** Kalthi, **b** ϕ 30.50 N- 33.10

30° 30' N–33° 6' N. The statistical analysis indicates that the results from cubic correlation (Eq. 17) have comparatively less variation than linear and quadratic equations. Thereby, cubic relations for other sites have also been developed. The developed correlations for the selected sites and their corresponding statistical analysis are presented in Table 8. A comparison of the calculated values with the optimum angle equations is shown in Fig. 10a for Kalthi and Fig. 10b for 30° 30' N–33° 6' N. Figure 10b advocates the precise estimation of yearly optimum tilt angle by Eq. 18 and Eq. 19, however, a comparatively large deviation of the results from Eq. 20. The reason for this deviation could be due to noisy estimates of higher-degree polynomial equations [45]. No such large deviations are observed for monthly optimum

tilt angle estimating equations (Eqs. 15–17) from Fig. 10a. Therefore, the developed correlations are significantly effective both statistically and graphically for precise estimation of monthly and yearly optimum tilt angles.

Comparison for correlation models: present study, previous works, NASA and PVGIS

The comparison of the developed mathematical models with the previously developed correlations and solar datasets like NASA and PVGIS has been presented in this section. NASA data were obtained from the NASA Langley Research Center (LaRC) POWER Project, funded through the NASA Earth Science /Applied Science Program [36]. PVGIS data have

Table 9 Comparison of current results with previous studies

Location	Latitude	Longitude	Solar data		Developed models		Previous models							
			NASA	PVGIS	Equation 18	Equation 19	Equation 20	[26]	[29]	[41]	[47]	[48]	[49]	[50]
Manpur Devra	30° 27' 9.648"	77° 40' 48"	28.00	33.00	27.70	27.66	27.86	25.44	33.93	28.57	27.31	28.29	27.03	31.45
Kalth	30° 51' 1.656"	77° 3' 36"	28.50	33.00	28.06	28.02	28.25	25.75	34.26	28.92	27.53	28.66	27.38	31.77
Kunihar	31° 4' 42.456"	76° 57' 36"	28.50	33.00	28.24	28.20	28.44	25.90	34.42	29.10	27.64	28.84	27.56	31.93
Bahali Dhar	31° 25' 27.696"	77° 42' 0"	29.00	33.00	28.51	28.47	28.72	26.13	34.67	29.36	27.80	29.11	27.82	32.17
Kalpa	31° 32' 25.08"	78° 14' 24"	29.50	31.00	28.60	28.56	28.82	26.21	34.75	29.45	27.85	29.21	27.91	32.25
Barot	32° 2' 11.544"	76° 50' 24"	29.50	31.00	29.05	29.01	29.28	26.59	35.16	29.89	28.12	29.67	28.35	32.65
Shallin	32° 12' 15.372"	77° 7' 48"	31.00	32.00	29.23	29.19	29.46	26.74	35.33	30.07	28.22	29.85	28.53	32.81
Rangrik	32° 14' 48.156"	78° 1' 48"	32.00	25.00	29.23	29.19	29.46	26.74	35.33	30.07	28.22	29.85	28.53	32.81
Hughal	33° 5' 33.216"	76° 24' 0"	31.50	28.00	30.05	30.00	30.25	27.43	36.07	30.87	28.69	30.67	29.32	33.50
Nalagarh	31° 1' 34.176"	76° 40' 57"	28.50	32.00	28.15	28.11	28.34	34.34	29.01	27.58	28.75	27.47	31.85	25.82

been developed for more than 10 years at the European Commission Joint Research Center at the JRC facility in Ispra, Italy [46]. The comparison is presented in Table 9. Tilt angle (β) values give rational results when the comparison data of different methods are examined. The comparison of previously developed models from the literature [47–50], solar datasets (NASA, PVGIS) and the present study signify that the optimum tilt angle suggested by developed models is significantly different from the other studies and effective as well. Thereby, the utilization of developed models will facilitate more benefit over the previously developed correlations and solar datasets.

Conclusions

The current article discusses the monthly and yearly optimum tilt angle assessment for solar plant setup-able sites in the Western Himalayas region. Experimental validation of the estimated optimum tilt angles has been conducted, and correlations have been developed. Following broad conclusions can be drawn from this study.

- (1) The monthly optimum tilt angle varies from 0° to 56° throughout the year for selected sites. The minimum and maximum values of monthly optimum angle have been observed for May–July and December, respectively.
- (2) Annual average percentage performance enhancement (AAPPE) for solar collector tilted at monthly optimum tilt angle is 10–11%, 5–7% and 4–6% from solar collector fitted at horizontal, equal to latitude angle and yearly optimum tilt angle, respectively. Results depict that the optimum tilt angle significantly improves the solar radiation collection rate.
- (3) Validation of results has been conducted through experimental analysis. Power output performance enhancement (POPE) for PV panel tilted at monthly optimum tilt angle from horizontal, tilted at the latitude and yearly optimum tilt angle has been calculated. The percentage variation of POPE from the performance enhancement (PE) for one of the selected locations is found to be 8.84, 14.09 and 9.13 for $\beta = 0^\circ$, $\beta = \beta_{opt}$, yearly and $\beta = \phi$, respectively.
- (4) Correlation development (linear, quadratic and cubic polynomial equations) for the selected region based on latitude (30° 30' N– 33° 6' N) and declination angles (for $\phi = 30^\circ 51' 1.656''$ N) has been conducted. The statistical analyses indicate that developed mathematical models are significantly applicable in the Western Himalayas region.
- (5) The applicability of the developed mathematical models has been checked by the comparison of results from

previously developed correlations and solar datasets (NASA and PVGIS). The intimacy of the current study results with the previously developed correlations, and solar datasets signifies the accuracy and applicability of the developed models for selected sites.

This study demonstrates the significance of optimum tilt angle assessment, their experimental validation and correlation development. This study would be useful for setting up a solar power plant at any suggested location.

Acknowledgements The authors would like to acknowledge NASA for providing SSE datasheets of solar insolation and Green Hills Polytechnic, Solan, for providing experimentation facilities.

Author contributions AA helped in conceptualization, data curation, formal analysis, investigation, writing—original draft. MK contributed to data curation, formal analysis, visualization, methodology, writing—original draft. AS performed conceptualization, data curation, formal analysis, investigation, methodology, writing—original draft, writing—review & editing. AM helped in formal analysis, resources, writing—review & editing. RC was involved in methodology, formal analysis, resources, supervision, writing—review & editing. TS helped in conceptualization, formal analysis, investigation, writing—original draft, writing—review & editing.

Funding Open access funding provided by Eötvös Loránd University.

Open Access This article is licensed under a Creative Commons Attribution 4.0 International License, which permits use, sharing, adaptation, distribution and reproduction in any medium or format, as long as you give appropriate credit to the original author(s) and the source, provide a link to the Creative Commons licence, and indicate if changes were made. The images or other third party material in this article are included in the article's Creative Commons licence, unless indicated otherwise in a credit line to the material. If material is not included in the article's Creative Commons licence and your intended use is not permitted by statutory regulation or exceeds the permitted use, you will need to obtain permission directly from the copyright holder. To view a copy of this licence, visit <http://creativecommons.org/licenses/by/4.0/>.

References

- Rani P, Tripathy PP. Heat transfer augmentation of flat plate solar collector through finite element-based parametric study. *J Therm Anal Calorim.* 2022;147:639–60.
- Sudhakar P, Cheralathan M. Thermal performance enhancement of solar air collector using a novel V-groove absorber plate with pin-fins for drying agricultural products: an experimental study. *J Therm Anal Calorim.* 2020;140:2397–408.
- Gilani HA, Hoseinzadeh S. Techno-economic study of compound parabolic collector in solar water heating system in the northern hemisphere. *Appl Therm Eng.* 2021;190:116756.
- Hoseinzadeh S, Garcia DA. Techno-economic assessment of hybrid energy flexibility systems for islands' decarbonization: a case study in Italy. *Sustain Energy Technol Assess.* 2022;51:101929.
- Kabir E, Kumar P, Kumar S, Adelodun AA, Kim K-H. Solar energy: potential and future prospects. *Renew Sustain Energy Rev.* 2018;82:894–900.
- Annual Report 2017–18 [Internet]. The ministry of new and renewable energy, Govt. of India; 2018. <https://mnre.gov.in/knowledge-center/publication>
- Khodayar Sahebi H, Hoseinzadeh S, Ghadamian H, Ghasemi MH, Esmailion F, Garcia DA. Techno-economic analysis and new design of a photovoltaic power plant by a direct radiation amplification system. *Sustainability.* 2021;13:11493.
- Shakouri M, Ghadamian H, Hoseinzadeh S, Sohani A. Multi-objective 4E analysis for a building integrated photovoltaic thermal double skin Façade system. *Sol Energy.* 2022;233:408–20.
- Sohani A, Hoseinzadeh S, Samiezadeh S, Verhaert I. Machine learning prediction approach for dynamic performance modeling of an enhanced solar still desalination system. *J Therm Anal Calorim.* 2022;147:3019–30.
- Sohani A, Dehnavi A, Sayyaadi H, Hoseinzadeh S, Goodarzi E, Garcia DA, et al. The real-time dynamic multi-objective optimization of a building integrated photovoltaic thermal (BIPV/T) system enhanced by phase change materials. *J Energy Storage.* 2022;46:103777.
- Khan Y, Soudagar ME, Kanchan M, Afzal A, Banapurmath N, Akram N, et al. Optimum location and influence of tilt angle on performance of solar PV panels. *J Therm Anal Calorim.* 2020;141:511–32.
- Calabrò E. An algorithm to determine the optimum tilt angle of a solar panel from global horizontal solar radiation. *J Renew Energy.* 2013;2013:1–12.
- Thakur V, Chandel SS. Maximizing the solar gain of a grid-interactive solar photovoltaic power plant. *Energy Technol.* 2013;1:661–7.
- Awasthi A, Mohan A, Sharma A. Tilt angle optimization and formulation of annual adjustment models for a solar power plant setup-able site at Himachal Pradesh, India. *Int J Innov Technol Explor Eng.* 2020;9:1181–5.
- Abdolzadeh M, Mehrabian MA. Obtaining maximum input heat gain on a solar collector under optimum slope angle. *Int J Sustain Energy.* 2011;30:353–66.
- Benghanem M. Optimization of tilt angle for solar panel: case study for Madinah. *Saudi Arabia Appl Energy.* 2011;88:1427–33.
- De Bernardes LS, Buitrago RH, Garcia NO. Photovoltaic generated energy and module optimum tilt angle from weather data. *Int J Sustain Energy.* 2011;30:311–20.
- Abdulsalam A, Idris AB, Ahmad T, Ahsan A. Radiation modeling and performance evaluations of fixed, single- and double-axis tracking surfaces: a case study for Dhahran city. *Saudi Arabia Int J Sustain Energy.* 2017;36:61–77.
- Soulayman S, Sabbagh W. Optimum tilt angle at tropical region. *Int J Renew Energy Dev. Center of Biomass & Renewable Energy, Dept. of Chemical Engineering, Diponegoro University;* 2015; 4:48–54
- Gharakhani Siraki A, Pillay P. Study of optimum tilt angles for solar panels in different latitudes for urban applications. *Sol Energy.* 2012;86:1920–8.
- Shukla KN, Rangnekar S, Sudhakar K. Comparative study of isotropic and anisotropic sky models to estimate solar radiation incident on tilted surface: a case study for Bhopal. *India Energy Rep.* 2015;1:96–103.
- Sharma A, Kallioğlu MA, Awasthi A, Chauhan R, Fekete G, Singh T. Correlation formulation for optimum tilt angle for maximizing the solar radiation on solar collector in the Western Himalayan region. *Case Stud Therm Eng.* 2021;26:101185.
- Ajao K, Ambali RM, Mahmoud M. Determination of the optimal tilt angle for solar photovoltaic panel in Ilorin. *Nigeria J Eng Sci Tech Rev.* 2013;6:87–90.
- Othman AB, Belkilani K, Besbes M. Global solar radiation on tilted surfaces in Tunisia: measurement, estimation and gained energy assessments. *Energy Rep.* 2018;4:101–9.

25. Yadav P, Chandel SS. Comparative analysis of diffused solar radiation models for optimum tilt angle determination for Indian locations. *Appl Sol Energy*. 2014;50:53–9.
26. Wessley GJJ, Starbell RN, Sandhya S. Modelling of optimal tilt angle for solar collectors across eight Indian cities. *Int J Renew Energy Res*. 2017;7:6.
27. Yadav AK, Chandel SS. Formulation of new correlations in terms of extraterrestrial radiation by optimization of tilt angle for installation of solar photovoltaic systems for maximum power generation: case study of 26 cities in India. *Sādhanā*. 2018;43:81.
28. Yadav AK, Malik H. Optimization of tilt angle for installation of solar photovoltaic system for six sites in India. 2015 Int Conf Energy Econ Environ ICEEE [Internet]. Greater Noida, India: IEEE; 2015, p 1–4. <http://ieeexplore.ieee.org/document/7235078/>. Accessed 21 Jun 2020
29. Stanciu C, Stanciu D. Optimum tilt angle for flat plate collectors all over the World—a declination dependence formula and comparisons of three solar radiation models. *Energy Convers Manag*. 2014;81:133–43.
30. Pourgharibshahi H, Abdolzadeh M, Fadaeinedjad R. Verification of computational optimum tilt angles of a photovoltaic module using an experimental photovoltaic system. *Environ Prog Sustain Energy*. 2015;34:1156–65.
31. Chandel M, Agrawal GD, Mathur S, Mathur A. Techno-economic analysis of solar photovoltaic power plant for garment zone of Jaipur city. *Case Stud Therm Eng*. 2014;2:1–7.
32. Annual Report 2019–20 [Internet]. The ministry of new and renewable energy, Govt. of India; 2018. <https://mnre.gov.in/knowledge-center/publication>
33. State of Forest Report. Forest Survey of India; 2017
34. Wastelands Atlas of India. Department of Land resources, ministry of rural development, Govt. of India; 2019
35. Google Maps [Internet]. Google Maps. <https://www.google.com/maps>. Accessed 10 Feb 2022
36. POWERIData Access Viewer [Internet]. <https://power.larc.nasa.gov/data-access-viewer/>. Accessed 9 Feb 2022
37. Ramachandra TV, Krishnadas G, Jain R. Solar potential in the Himalayan landscape. *Int Sch Res Not*. 2012. <https://doi.org/10.5402/2012/203149>.
38. Duffie JA, Beckman WA, Blair N. *Solar engineering of thermal processes, photovoltaics and wind*. 5th ed. Hoboken: Wiley; 2020.
39. Liu B, Jordan R. Daily insolation on surfaces tilted towards equator. *ASHRAE J United States*. 1961;10.
40. Kallioğlu MA, Durmuş A, Karakaya H, Yılmaz A. Empirical calculation of the optimal tilt angle for solar collectors in northern hemisphere. *Energy Sour Part Recovery Util Environ Eff*. 2020;42:1335–58.
41. Stone RJ. Improved statistical procedure for the evaluation of solar radiation estimation models. *Sol Energy*. 1993;51:289–91.
42. Besharat F, Dehghan AA, Faghhih AR. Empirical models for estimating global solar radiation: a review and case study. *Renew Sustain Energy Rev*. 2013;21:798–821.
43. Bakirci K. Correlations for optimum tilt angles of solar collectors: a case study in Erzurum, Turkey. *Energy Sour Part Recovery Util Environ Eff*. 2012;34:983–93.
44. Ulgen K. Optimum tilt angle for solar collectors. *Energy Sour Part Recovery Util Environ Eff*. 2006;28:1171–80.
45. Gelman A, Imbens G. Why high-order polynomials should not be used in regression discontinuity designs. *J Bus Econ Stat*. 2019;37:447–56.
46. JRC Photovoltaic Geographical Information System (PVGIS)—European Commission Internet. https://re.jrc.ec.europa.eu/pvg_tools/en/tools.html#MR. Accessed 23 Oct 2019
47. Jacobson MZ, Jadhav V. World estimates of PV optimal tilt angles and ratios of sunlight incident upon tilted and tracked PV panels relative to horizontal panels. *Sol Energy*. 2018;169:55–66.
48. Moghadam H, Tabrizi FF, Sharak AZ. Optimization of solar flat collector inclination. *Desalination*. 2011;265:107–11.
49. Darhmaoui H, Lahjouji D. Latitude based model for tilt angle optimization for solar collectors in the Mediterranean region. *Energy Procedia*. 2013;42:426–35.
50. Chang TP. The Sun's apparent position and the optimal tilt angle of a solar collector in the northern hemisphere. *Sol Energy*. 2009;83:1274–84.

Publisher's Note Springer Nature remains neutral with regard to jurisdictional claims in published maps and institutional affiliations.